JOURNAL OF APPLIED ELECTROCHEMISTRY **28** (1998) 827–834

Oxygen reduction on bornite (Cu_5FeS_4) in alkaline medium

J. L. GAUTIER*, J. ORTIZ

Laboratorio de Electroquimica, Departamento de Quimica de Materiales, Faculdad de Quimica y Biologia, Universidad de Santiago de Chile, C.C 33040, Santiago, Chile

N. HELLER-LING, G. POILLERAT, P. CHARTIER

Laboratoire d'Electrochimie et Chimie-Physique du Corps Solide, Faculté de Chimie, URA CNRS 405, Université Louis Pasteur, rue Blaise Pascal, 67000 Strasbourg, France

Received: 7 April 1997; revised 12 January 1998

The electroreduction of molecular oxygen is investigated between −0.1 and −0.5 V vs SHE on bornite, Cu_5FeS_4, at pH 9.2 and 14, by means of cyclic voltammetry (CV) and stationary voltammetry (SV), using a double channel electrode flow cell (DCEFC). Using an E/pH diagram established in this work, the CV results suggest that the bornite surface is stable between −0.1 and −0.5 V then oxidized to CuS and $Fe(OH)_3$ above −0.1 V whereas, below −0.5 V the mineral reduces to metal sulphides: Cu_2S and FeS. The SV results show that oxygen is reduced to peroxide ions, HO_2^-. At pH 9.2 the generated sulphide ions hinder the oxidation of HO_2^- on the collector electrode of the DCEFC, due to the formation of a blocking surface layer of elemental sulphur, S, impeding the determination of the kinetic parameters, k_1 (direct way) and k_2 (indirect way) of the oxygen electroreduction reaction. In contrast, at pH 14, as soluble polysulphides are formed, it was possible to determine these parameters, showing that the bornite is a poor catalyst for oxygen reduction. At pH 14, in the presence of potassium ethylxanthate, generally used as a flotation collector, the ethylxanthate ions, $C_2H_5OCSSO^-$, are oxidized by HO_2^- to perxanthates, $ROCSSO^-$, while at pH 9.2 the oxygen reduction is inhibited due to ethylxanthate chemisoption on the bornite surface.

Keywords: *alkaline medium*, *bornite*, *double channel flow cell*, *oxygen reduction*

1. Introduction

Concentration of minerals by flotation uses the natural surface hydrophobicity of solid particles or enhances it by means of specific surfactants, or collectors, such as dialkyldithiocarbamates, R_2NCSS^-, or alkylxanthates, $ROCSS^-$. The interaction between the collector and the particle conditions the flotation process [1]. Investigations on various sulphide–xanthate couples have demonstrated that the presence of air is necessary since, in addition to mineral separation from the gang, oxygen, which participates in the overall adsorption mechanism, is electrochemically reduced [2, 3].

The electrochemical reduction of molecular oxygen in alkaline medium is a complex reaction which involves two parallel pathways [4]. Oxygen molecules are reduced either directly to hydroxyl ions, OH^-, using 4 e^- per oxygen molecule or, indirectly, through two consecutive reactions, each of these reactions transferring 2 e^- and the first one generating intermediate hydrogen peroxide ions, HO_2^-, (see Section 3.2). The contribution of each pathway is usually determined by means of a rotating ring disc electrode (RRDE) technique, whose hydrodynamics is well known [5]. Recently, alternative techniques have been developed allowing for other electrode geometries, in tubular or duct type cells in which, in contrast to the RRDE, the electrodes are static and the electrolyte is flowing. One of these techniques use the double channel electrode flow cell (DCEFC), whose theory has been developed by Compton and Unwin [6].

Investigations in alkaline medium on sulphide minerals (pyrite, for instance), using the RRDE, have showed that the electroreduction of oxygen occurs mainly via the indirect pathway, and that traces of HO_2^- are sufficient to oxidize the xanthate collector [2], diminishing the flotation yield, [7–9]. For this reason, understanding of the mechanism of oxygen electroreduction on sulphide minerals is important in the flotation process.

The present work reports a preliminary study of oxygen electroreduction on bornite, Cu_5FeS_4, at pH 9.2 and pH 14, using a DCEFC.

2. Experimental details

Single crystals of bornite, Cu_5FeS_4, from El Salvador, Chile, were used. X-ray diffractometry showed the lines and relative intensities corresponding exactly to

* Author to whom correspondence should be addressed.

PDF 42-1405, spatial group Fm3m. X-ray fluorescence analyses showed only low levels of calcium and lead impurities.

Electrochemical measurements consisted in recording either cyclic voltammograms at the generator electrodes of the DCEFC or simultaneously steady state voltammograms at the generator and collector electrodes. These were obtained using a Tacussel Bi-Pad potentiostat and an Ifelec IF 6700 X–Y recorder. The design of the DCEFC has been fully described elsewhere [10]. In this work the generator electrode was a parallelepipedic bornite crystal (10 mm × 2.5 mm × 2 mm) with an exposed apparent surface area of 0.25 cm^2 and the collector electrode was a platinum plate. The channel, along which the electrolyte flowed, was 10 cm × 3 cm × 0.1 cm. The generator to collector area ratio was 1:15, the distance between the electrodes being 0.11 mm downstream. The collection efficiency factor was $N = 0.55$. The products of the oxygen electroreduction on the generator electrode are oxidized on the collector electrode. Before each measurement, the bornite crystal was polished using silicon carbide papers (Norton) 800, 1000 and 1200. The platinum collector was polished using diamond paste (Escil Aerosol 1 PS4), 0.5 and 2 μm in grain size. Both electrodes were washed with large amounts of alcohol and distilled water. Electrolyte was fed through a peristaltic pump (Masterflex 7014-20) and the rate of flow was monitored from 1.0 to 10.6 mL min^{-1} using a bowl flowmeter (Cole Palmer 042-15 G).

The solutions were prepared from analytical grade KOH (Normapur, Prolabo) $Na_2B_4O_7, 10\,H_2O$ (Janssen Chimica) and potassium ethylxanthate, KC_2H_5OCSSO, 98% (Lancaster). Water was purified using ion exchange resins. Oxygen and nitrogen were used without additional purification. The electrolyte compositions were: 0.05 M $Na_2B_4O_7$ (pH 9.2), 1 M KOH (pH 14) and recrystallized KC_2H_5OCSS 0.01% w/o. The xanthate solutions were prepared daily to avoid decomposition.

The reference electrode used was the Hg/HgO/KOH(1 M) electrode (E = 0.098 V vs SHE). The potentials indicated in this work are reported on the SHE scale.

3. Results and discussion

3.1. *Cu_5FeS_4 stability*

The stability of Cu_5FeS_4 crystal was investigated by CV prior to the study of oxygen reduction by SV on this electrode.

Figure 1 shows two cyclic voltammetric curves E/I, recorded at a scan rate of 40 mV s^{-1}, between 0 and −0.6 V, at the Cu_5FeS_4 generator electrode, corresponding to the response of the bornite surface under cyclic polarization in nitrogen saturated solutions at pH 9.2 and 14 (curves 1 and 2, respectively). A capacitive current of the same intensity for both pH, occurs from −0.07 to −0.5 V. When the positive-going

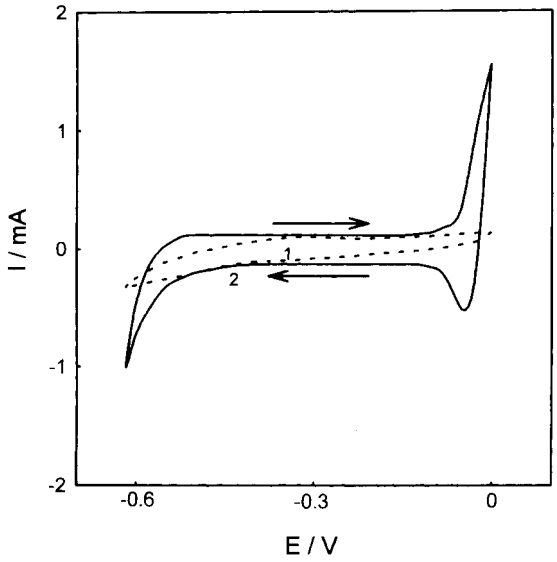

Fig. 1. Cyclic voltammetry of bornite in aqueous solution saturated with N_2. (1) pH 9.2 (2) pH 14; scanning rate: 40 mV s^{-1}; $E_{j=0} = -0.1$ V.

scan was continued beyond −0.07 V, the anodic current increases at pH 14 but not at pH 9.2 due to the oxidation of the bornite surface in accordance with the following reaction [11, 12]: $Cu_5FeS_4 + 3\,H_2O \rightarrow Cu_5S_4 + Fe(OH)_3 + 3\,H^+ + 3\,e^-$. At pH 9.2 this reaction occurs at about 0 V because the shift is governed by 59 mV per pH unit as reported by Buckley *et al.* [11]. When the potential scan was reversed in the negative direction, a cathodic peak at −0.05 V was detected (Fig. 1). The anodic peak charge is greater than the cathodic one (obtained by integration) which suggests that the above reaction is not reversible. Some soluble species such as CuO_2^{2-}, $CuOH^+$, or $Cu_2(OH)_2^{2+}$ have been detected [12].

Thermodynamic considerations gave rise to the construction of the E/pH diagram of bornite shown in Fig. 2. The diagram was established by the present

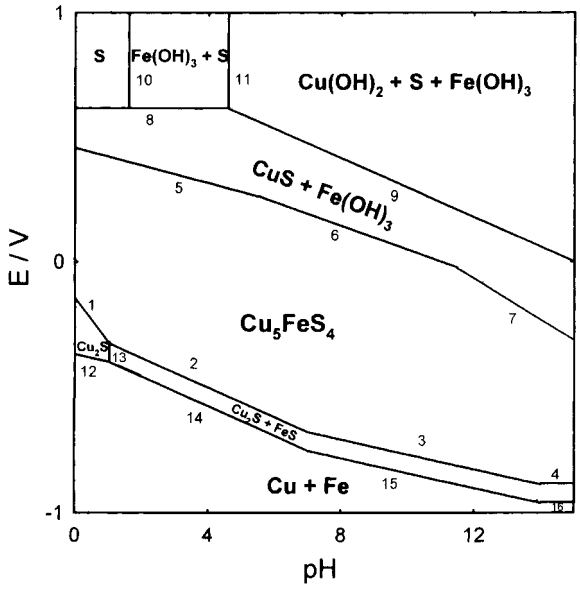

Fig. 2. Potential–pH diagram of bornite, Cu_5FeS_4. The arabic numbers are related to the electrochemical and chemical reactions signaled on Table 2.

Table 1. Thermodynamic data used for Fig. 2.

Ions in solution	ΔG_f^0/kJ mol^{-1}	*Ref.*
H^+	0	[13]
H_2O	−236.96	[13]
Cu^{2+}	64.92	[13]
CuO_2^{2-}	−181.83	[13]
$Cu_2(OH)_2^{2+}$	−280.06	[16]
Fe^{2+}	−84.85	[13]
Fe^{3+}	−10.57	[13]
$H_2S_{(aq)}$	−27.34	[13]
HS^-	12.58	[13]
S^{2-}	91.79	[13]
Solids	ΔG_f^0/kJ mol^{-1}	*Ref.*
Cu_5FeS_4	−353.34	estimated from [14]
Cu_2S	−85.48	[16]
CuS	−53.88	[16]
$Cu(OH)_2$	−356.55	[13]
$Fe(OH)_3$	−693.88	[13]
FeS	−100.32	[15]
S orthorhombic	0	

Table 3. pH and E/pH equations used in Fig. 2.

$$E_0 = -0.143 - 0.177\ \mathrm{pH} - 0.0591\ \log(Fe^{2+}) - 0.0885\ \log(H_2S) \quad (1)$$

$$E_0 = -0.266 - 0.0591\ \mathrm{pH} - 0.0296\ \log(H_2S) \quad (2)$$

$$E_0 = -0.473 - 0.0296\ \mathrm{pH} - 0.0296\ \log(HS^-) \quad (3)$$

$$E_0 = -0.884 - 0.0296\ \log(S^{2-}) \quad (4)$$

$$E_0 = 0.455 - 0.0355\ \mathrm{pH} + 0.011\,82\ \log(Cu^{2+}) \quad (5)$$

$$E_0 = 0.522 - 0.0827\ \mathrm{pH} + 0.011\,82\ \log(Cu_2(OH)_2^{2+}) \quad (6)$$

$$E_0 = 0.926 - 0.0827\ \mathrm{pH} + 0.011\,82\ \log(CuO_2^{2-}) \quad (7)$$

$$E_0 = 0.616 + 0.0296\ \log(Cu^{2+}) \quad (8)$$

$$E_0 = 0.887 - 0.0591\ \mathrm{pH} \quad (9)$$

$$3\ \mathrm{pH} = -\log(Fe^{3+}) + 4.83 \quad (10)$$

$$E_0 = -0.370 - 0.0296\ \mathrm{pH} + 0.0148\ \log(Fe^{2+}) - 0.0148\ \log(H_2S) \quad (11)$$

$$E_0 = -0.547 - 0.0296\ \mathrm{pH} - 0.0296\ \log(HS^-) \quad (12)$$

$$2\ \mathrm{pH} = 2.08 - \log(Fe^{2+}) - \log(H_2S) \quad (13)$$

$$E_0 = -0.340 - 0.0591\ \mathrm{pH} - 0.0296\ \log(H_2S) \quad (14)$$

$$E_0 = -0.547 - 0.0296\ \mathrm{pH} - 0.0296\ \log(HS^-) \quad (15)$$

$$E_0 = -0.958 - 0.0296\ \log(S^{2-}) \quad (16)$$

authors taking into account (i) the thermodynamic data [13–16], shown in Table 1, (ii) a complete set of selected reactions (Table 2) and (iii) their respective E/pH equations (Table 3). The activities of all soluble species shown in Fig. 2 were taken as unity. Only the stable oxidation states −2 and 0 of sulphur were retained, discarding the higher oxidation states +4 and +6, whose formation is kinetically extremely slow [16]. The nonstoichiometric metastable sulphides [16–18] were also not considered.

In the following CV interpretation, reactions and equations numbers refer to reactions and equations in Fig. 2, Tables 2 and 3, respectively.

At pH 9.2 (curve 1, Fig. 1), the bornite surface begins to reduce at −0.45 V, with formation of Cu_2S, FeS, and HS^- (Reaction 3). Reaction 3 depends simultaneously on pH and on the activity of the HS^- ions (Equation 3, Table 3). On the reverse scan, bornite is regenerated at the same potential according to the inverted Reaction 3. In the case of pH 14 (curve 2, Fig. 1), the E/pH diagram indicates that bornite begins to reduce at −0.50 V with formation of Cu_2S, FeS and S^{2-} (Reaction 4). This reaction is pH independent. Bornite can be regenerated by the inverse Reaction 4. However, the oxidation occurs at −0.07 V with formation of CuS, $CuO_2^{2-}$and $Fe(OH)_3$ (inverted Reaction 7). The recombination of these reaction products on the reverse scan (Reaction 7), causes the pronounced cathodic peak around −0.05 V.

In conclusion, CV measurements show that bornite is stable (i) at pH 9.2, from 0 to −0.45 V, and (ii) at pH 14 between −0.1 V and −0.5 V. In these potential regions very low capacitive currents are observable (in the μA range).

Table 2. Chemical and electrochemical reactions used in Fig. 2.

$$2\,Cu_5FeS_4 + 6\,H^+ + 2\,e^- \rightarrow 5\,Cu_2S + 2\,Fe^{2+} + 3\,H_2S \quad (1)$$

$$2\,Cu_5FeS_4 + 2\,H^+ + 2\,e^- \rightarrow 5\,Cu_2S + 2\,FeS + H_2S \quad (2)$$

$$2\,Cu_5FeS_4 + H^+ + 2\,e^- \rightarrow 5\,Cu_2S + 2\,FeS + HS^- \quad (3)$$

$$2\,Cu_5FeS_4 + 2\,e^- \rightarrow 5\,Cu_2S + 2\,FeS + S^{2-} \quad (4)$$

$$5\,CuS + Cu^{2+} + Fe(OH)_3 + 5\,e^- \rightarrow Cu_5FeS_4 + 3\,H_2O \quad (5)$$

$$8\,CuS + Cu_2(OH)_2^{2+} + 2\,Fe(OH)_3 + 8\,H^+ + 10\,e^- \rightarrow 2\,Cu_5FeS_4 + 8\,H_2O \quad (6)$$

$$4\,CuS + CuO_2^{2-} + Fe(OH)_3 + 7\,H^+ + 5e^- \rightarrow Cu_5FeS_4 + 5\,H_2O \quad (7)$$

$$Cu^{2+} + S + 2\,e^- \rightarrow CuS \quad (8)$$

$$Cu(OH)_2 + S + 2\,H^+ + 2\,e^- \rightarrow CuS + 2\,H_2O \quad (9)$$

$$Fe(OH)_3 + 3\,H^+ \rightarrow Fe^{3+} + 3\,H_2O \quad (10)$$

$$Cu(OH)_2 + 2\,H^+ \rightarrow Cu^{2+} + 2\,H_2O \quad (11)$$

$$Cu_2S + Fe^{2+} + 2\,H^+ + 4\,e^- \rightarrow 2\,Cu + Fe + 2\,H_2S \quad (12)$$

$$FeS + 2\,H^+ \rightarrow Fe^{2+} + H_2S \quad (13)$$

$$Cu_2S + FeS + 4\,H^+ + 4\,e^- \rightarrow 2\,Cu + Fe + 2\,H_2S \quad (14)$$

$$Cu_2S + FeS + 2\,H^+ + 4\,e^- \rightarrow 2\,Cu + Fe + 2\,HS^- \quad (15)$$

$$Cu_2S + FeS + 4\,e^- \rightarrow 2\,Cu + Fe + 2\,S^{2-} \quad (16)$$

3.2. *Electroreduction of O_2 on bornite using the DCEFC*

The electroreduction of oxygen has been extensively investigated especially using the rotating disc electrode (RDE) and the rotating ring disc electrode (RRDE) [19–30]. Recently, we have reported on oxygen electroreduction on oxides using the double channel electrode flow cell (DCEFC) and the results have been interpreted on the basis of the reaction scheme shown in Fig. 3 [10, 31]. According to this scheme, which is also assumed to hold with sulphides, the reactions on the generator electrode, in alkaline medium, are:

Direct pathway

$$O_2 + 2\,H_2O + 4\,e^- \rightarrow 4\,OH^-$$
$$E^\circ = -0.401\ \mathrm{V\ vs\ SHE} \quad (1)$$

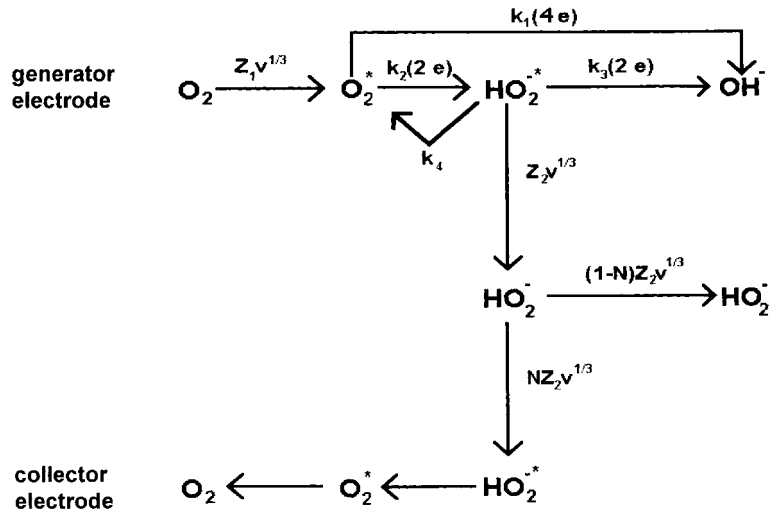

Fig. 3. Scheme of the oxygen reduction mechanism on surface electrode in alkaline medium [10, 31].

with kinetic constant k_1.

Indirect pathway

$$O_2 + H_2O + 2\,e^- \rightarrow HO_2^- + OH^- \qquad E^\circ = -0.065\ \text{V vs SHE} \tag{2a}$$

with kinetic constant k_2, followed by

$$HO_2^- + H_2O + 2\,e^- \rightarrow 3\,OH^- \qquad E^\circ = -0.867\ \text{V vs SHE} \tag{2b}$$

with kinetic constant k_3.

It is possible to accept a catalytic chemical decomposition of HO_2^- on the bornite surface:

$$HO_2^- \rightarrow OH^- + 1/2\ O_2 \tag{3}$$

with kinetic constant k_4.

The peroxide ions, HO_2^-, which are generated on the generator electrode, are reoxidized on the collector electrode according to the inverse of Reaction 2(a):

$$HO_2^- + OH^- \rightarrow O_2 + H_2O + 2\,e^-$$

The equations which describe the process recently reported are [31]:

$$-N\frac{I_g}{I_c} = \left[1 + \frac{2k_1}{k_2}\right] + \frac{1}{Z_{HO_2^-}v^{1/3}}\left[\frac{2k_1}{k_2}(k_3 + k_4) + (2k_3 + k_4)\right] \tag{4}$$

$$-N\frac{I_{g,lim} - I_g}{I_c} = \frac{n_g}{2}\left[\frac{D_{O_2}}{D_{HO_2^-}}\right]^{2/3}\left[\frac{k_3 + k_4}{k_2}\right] + \frac{n_g}{2}\frac{Z_{O_2}v^{1/3}}{k_2} \tag{5}$$

$$-\frac{I}{I_g} = -\frac{1}{I_{k,g}} + \frac{1}{n_g F S_g Z_{O_2} C_{O_2}}\left(\frac{1}{v^{1/3}}\right) \tag{6}$$

with $Z_i = 0.925\,D_i^{2/3}(hx_1)^{-1/3}$, $v = v_f/hd$, $I_{g,lim} = -n_g F S_g Z_{O_2} C_{O_2} v^{1/3}$, $I_{k,g} = -n_g F S_g k_g C_{O_2}$ and $k_g = k_1 + k_2$, N being the collection efficiency of the collector electrode, I_g and I_c the generator and collector currents, of opposite signs, F the Faraday constant, C_{O_2} the oxygen concentration, D_i the diffusion coefficient of a species i, i being O_2 or HO_2^-, n_g the mean number of electrons per oxygen molecule transferred at the generator electrode, S_g its geometric area, v_f the volumetric flux and v the flux velocity, d and h being the width and half height of the channel and x_1 the length of the generator electrode [10].

Regarding Equation 6, the number of electrons exchanged on bornite, n_g, may be obtained from the slope of $-1/I_g$ against $v^{-1/3}$ plots. The k_1/k_2 ratio can be obtained from the extrapolated ordinate at $v^{-1/3} = 0$ of $-NI_g/I_c$ against $v^{-1/3}$ plots (Equation 4), and k_2 from the slope of $-N(I_{g,lim} - I_g)/I_c$ against $v^{1/3}$ plots (Equation 5). From these values, it is possible to determine whether the reduction of oxygen proceeds via the direct reduction pathway (four electrons), via the indirect reduction pathway, in two steps (2 + 2 electrons), or simultaneously via both pathways (parallel mechanism), with predominance of one or the other pathway.

According to Section 3.1., the investigation of the reduction of oxygen on a Cu_5FeS_4 electrode has the following limitations: (i) the potential region of electrochemical inactivity of the electrode is very narrow since the oxygen reduction may occur at potentials at which the reduction of the mineral surface also occurs (Fig. 1), (ii) the reduction of the mineral surface generates HS^- ions (pH 9.2) or S^{2-} ions (pH 14), which are transported towards the collector electrode and oxidized simultaneously with the HO_2^- ions. The nature of the oxidation products depends on the pH and the applied potential. The oxidation of sulphur ions HS^-or S^{2-} in elemental sulphur, S, occurs through the intermediate formation of polysulphide ions, S_n^{2-}, with n between 2 and 5 [32, 33]. The S_n^{2-} ions contribute to the chemical dissolution of the sulphur film deposited on the electrode according to the following multiple equilibria [18]:

$$S + HS^- + OH^- \rightleftharpoons S_2^{2-} + H_2O;$$

$$S + S_2^{2-} \rightleftharpoons S_3^{2-}; \quad S + S_3^{2-} \rightleftharpoons S_4^{2-}; \quad S + S_4^{2-} \rightleftharpoons S_5^{2-}$$

Consequently, on the collector electrode, at pH 9.2, the layer of sulphur is more likely to be retained than at pH 14; this layer will prevent or inhibit the oxidation of HO_2^-. Elsewhere at pH 14, it is very likely that the S layer dissolves into S_n^{2+}.

Oxygen reduction on bornite using DCEFC was studied by means of E/I curves considering the following limitations:

(a) The E/I curves for oxygen reduction must be recorded in the potential range at which the reduction of the mineral surface is minimal.
(b) The S film formed on the collector electrode must be removed by oxidation to soluble species.
(c) According to condition b), SO_4^{2-} ions formation can be considered: $S + 4\,H_2O \rightarrow SO_4^{2-} + 8\,H^+ + 6\,e^-$. This reaction is depending to pH (0.0788 V/pH unit). Then, the potential applied to the collector electrode should be held at an $E = 0.38$ V more positive at pH 9.2 than at pH 14.
(d) HO_2^- oxidation process on the collector electrode must be controlled by diffusion. This condition has been experimentally obtained.
(e) The applied potential to oxidize the HO_2^- ions on the collector electrode cannot be very high, with the purpose of avoiding oxygen evolution that produces high background current, making the determination of the HO_2^- ions difficult.

The collector potential was fixed to 0.7 V because experimentally we found that maximum concentration of HO_2^- ions are obtained for both pH. The oxygen electrocatalysis current was corrected by the current due to the capacitive currents.

Figure 4 shows the steadystate E/I curves recorded at pH 9.2 and pH 14 between −0.1 V and −0.5 V on bornite in the absence and presence of oxygen using six different volumetric flow rates. In both cases the currents at the generator electrode, I_g, and at the collector electrode, I_c, are higher in oxygen saturated solutions than in deaerated solutions (absence of oxygen), principally due to oxygen electroreduction to HO_2^-. At pH 9.2, the currents I_g and I_c in deaerated or oxygen saturated solutions were not affected by the electrolyte flow, indicating that at this pH the electrochemical processes were not controlled by mass transport. Moreover, the I_c magnitude, lower than those obtained to pH 14, suggests that HS^- ions produced on the generator electrode were oxidized at the collector electrode into elemental S whose deposition affected the efficiency of collection of the HO_2^- ions detrimentally. In contrast, at pH 14, the current I_c is a function of v_f due to the diffusion control of HO_2^- and S^{2-} transport toward the electrode. The dependence of I_c on v_f can be also explained if it is assumed that S^{2-} is oxidized into S_n^{2-} and SO_4^{2-} on the collector electrode.

Due to the absence of diffusion control at pH 9.2, the pH 14 set of E/I curves was considered as being representative of oxygen interaction with the bornite surface in alkaline medium.

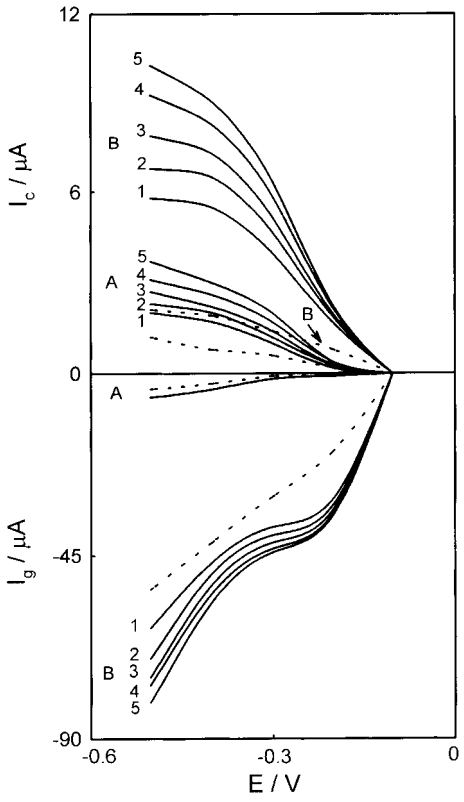

Fig. 4. Reduction of oxygen on bornite: (A) deaerated solution. (B) O_2 saturated solution for different volumetric fluxes: (1) 3.3; (2) 5; (3) 6.8; (4) 8.7 and (5) 10.6 mL min^{-1}. Scanning rate: 5 mV s^{-1}. pH 9.2 (dashed lines), pH 14 (full lines). I_g = generator current; I_c = collector current

Figure 5 shows the dependence on E of the reduction currents on the generator electrode (corrected for the capacitive currents, Fig. 4) and of the oxidation currents on the collector electrode (corrected for the oxidation of S^{2-} into SO_4^{2-}, Fig. 4). After these corrections, the former currents are representative of the reduction of oxygen and the latter of the oxidation of the intermediate HO_2^- ions, both currents being controlled by mass transport, according to the scheme on Fig. 3.

Figure 6 displays the $-1/I_g$ against $v^{-1/3}$ plots obtained from Fig. 5. From the slopes of the straight lines, which are equal to $1/n_g F Z_{O_2} S_g C_{O_2}$, it was possible to determine n_g. Using the following values: $F = 96\,490$ C mol^{-1}, $Z_{O_2} = 0.925\,D_{O_2}^{2/3}(hx_1)^{-1/3} = 1.17 \times 10^{-4}(m\,s^{-1})^{2/3}$, (with $h = 0.5 \times 10^{-3}$ m and $x_1 = 2.5 \times 10^{-3}$ m), $S_g = 2.5 \times 10^{-5}\,m^2$, $D_{O_2} = 15.9 \times 10^{-10}\,m^2\,s^{-1}$ [24], and $C_{O_2} = 0.89\,mol\,m^{-3}$ [24], n_g is computed to have a value of 2 at any potential between −0.3 V and −0.5 V, as indicated by the parallelism of the lines. Therefore, oxygen reduction proceeds mainly to HO_2^- only, using an average of $2\,e^-$ per O_2 molecule.

The plots of $-NI_g/I_c$ against $v^{-1/3}$ are shown in Fig. 7. The linearity of the plots is indicative of a reaction order unity in oxygen concentration [28, 29]. From the extrapolated ordinates at $v^{-1/3} = 0, k_1/k_2$ values were obtained. Figure 8 shows the plots of $-N(I_{g,lim} - I_g)$ against $v^{1/3}$. From the slopes of the plots, values for k_2 were obtained.

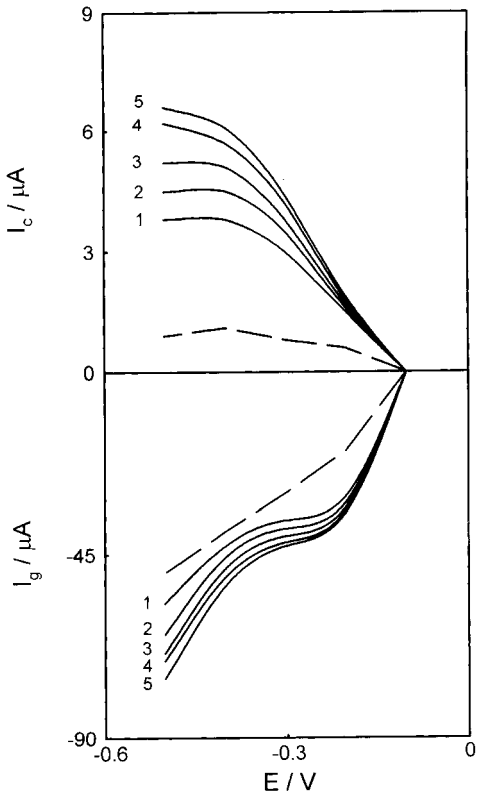

Fig. 5. Reduction of oxygen on bornite at pH 9.2 (dashed lines) and at pH 14 (full lines) for different volumetric fluxes: (1) 3.3; (2) 5.0; (3) 6.8; (4) 8.7 and (5) 10.6 mL min^{-1}. Curves corrected of the capacitive currents.

Table 4 gathers the kinetic information thus obtained. It is clear that the electroreduction of oxygen bornite at pH 14 occurs predominantly with formation of HO_2^-, compared to the parallel 4 e$^-$ reduction to OH^-, as $n_g = 2$ and $k_1/k_2 < 1$. The smaller magnitudes of the kinetic constants k_1 and k_2 show that the bornite surface behaves as a poor electrocatalyst for oxygen reduction compared, for instance, with catalytic metallic oxides [10, 31].

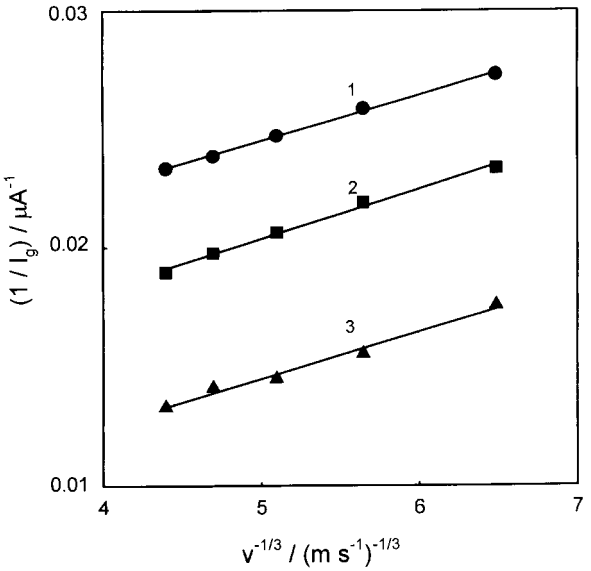

Fig. 6. $-1/I_g$ plot in function of $v_f^{-1/3}$, calculated from the data in Fig. 5, at three potentials applied: (1) −0.3; (2) −0.4 and (3) −0.5 V.

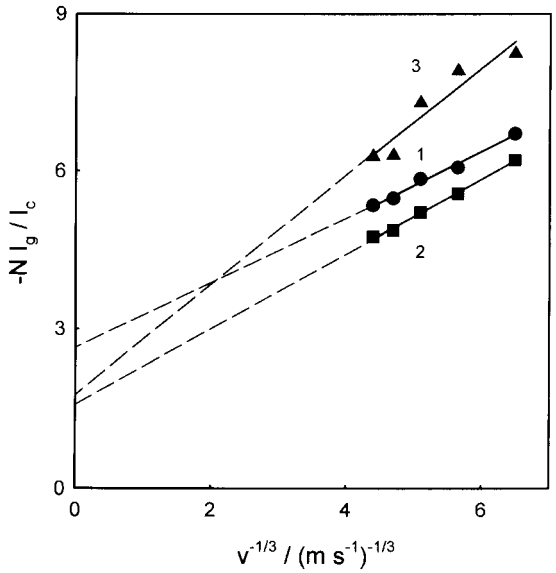

Fig. 7. $-NI_g/I_c$ plot as a function of $v_f^{-1/3}$, calculated from the data in Fig. 5, at (1) −0.3; (2) −0.4 and (3) −0.5 V.

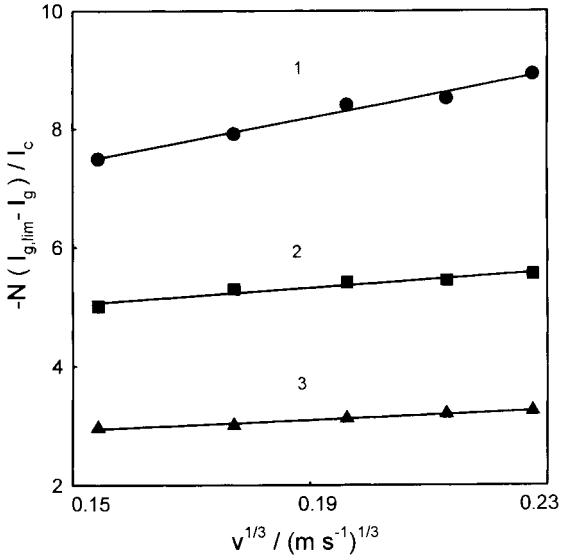

Fig. 8. $-N(I_{g,lim} - I_g)/I_c$ plot as a function of $v_f^{-1/3}$, calculated from the data in Fig. 5, at (1) −0.3; (2) −0.4 and (3) −0.5 V.

3.3. *Reduction of O_2 on bornite in the presence of ethylxanthate*

It is known that oxygen oxidises the alkylxanthate ions, $ROCSS^-$, into insoluble dixanthogen, $(ROCSS)_2$, on Pt, Au, Cu, Hg and ZnS [34, 35], according to Reaction 7:

$$2\,ROCSS^- + 1/2\,O_{2(ads)} + H_2O \rightarrow (ROCSS)_2 + 2\,OH^- \qquad (7)$$

Table 4. Kinetic parameters obtained from Figs 6, 7 and 8

E/V	−0.3	−0.4	−0.5
n_g	2	2	2
k_1/k_2	0.76	0.31	0.37
k_2 (m s^{-1}) × 10^5	1.2	3.4	5.6
k_1 (m s^{-1}) × 10^5	0.9	1.0	2.1

which occurs on the surface of the mineral similarly to a corrosion reaction, in the sense that charge transfer occurs via the conducting solid phase, [36].

Dissolved oxygen does not oxidise the $ROCSS^-$ ions homogeneously the reaction being kinetically slow [37], though being thermodynamically feasible. In alkaline medium, pH 11, the alkyldixanthogene $(ROCSS)_2$ decomposes to monothiocarbonate [38]. However in oxidizing alkaline medium, it is converted to xanthate, monothiocarbonate, perxanthate, [38], according to Reaction 8:

$$2(ROCSS)_2 + 6\,OH^- \rightarrow ROCSS^- + 2\,ROCSO^- + ROCSSO^- + S + S^{2-} + H_2O \quad (8)$$

The formation of the perxanthate ion, reaction 9, is favoured by the presence of high concentrations of HO_2^- generated by the reduction of oxygen, and also by the decomposition of the dixanthogen according to Reaction 10:

$$ROCSS^- + HO_2^- \rightarrow ROCSSO^- + OH^- \quad (9)$$

$$(ROCSS)_2 + 3\,OH^- \xrightarrow{\text{slow}} 2\,ROCSS^- + HO_2^- + H_2O \quad (10)$$

At pH 9.2, the dixanthogen is stable, since Reaction 10 is extremely slow compared to the formation of monothiocarbonate, Reaction 11:

$$(ROCSS)_2 + 4\,OH^- \xrightarrow{\text{fast}} 2\,ROCSO^- + S + S^{2-} + 2\,H_2O \quad (11)$$

Figure 9 shows the E/I curves for oxygen reduction on bornite, corrected as in Fig. 5 and recorded at pH 9.2 and pH 14 in the presence of 1×10^{-6} mol dm^{-3} potassium ethylxanthate. At pH 9.2, I_g is slightly lower than without ethylxanthate whereas I_c has the same magnitude (see Fig. 5). As in absence of ethylxanthate, I_c and I_g were insensitive to the flow velocity, probably due to the inhibition of oxygen reduction by ethylxanthate chemical adsorption on the bornite and the oxidation of the xanthate ion to insoluble dixanthogen, which blocked the collector electrode surface. At pH 14, oxygen reduction and HO_2^- oxidation were again controlled by mass transport, the currents being sensitive to flow velocity. The currents on the generator electrode, I_g, were greater than in the absence of xanthate and showed a cathodic peak at about −0.2 V, probably due to ethylxanthate adsorption [12]. The currents on the collector electrode, I_c, also were higher, which suggests that the dixanthogen is dissolved and oxidized as described above.

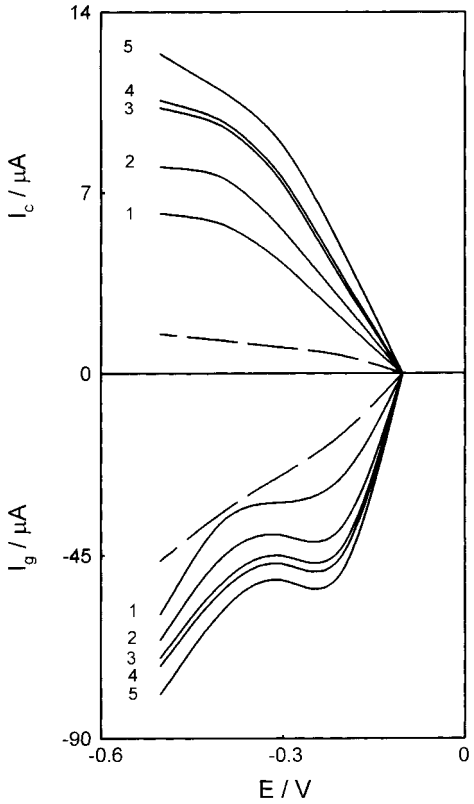

Fig. 9. Reduction of oxygen on bornite in presence of potassium ethylxanthate 1×10^{-6} mol dm^{-3} at (- - -) pH 9.2 and (——) at pH 14 for different volumetric fluxes: (1) 3.3; (2) 5.0; (3) 6.8; (4) 8.7 and (5) 10.6 mL min^{-1}.

4. Conclusion

The electrochemical reduction of molecular oxygen on bornite, Cu_5FeS_4, has been conveniently investigated between −0.1 and −0.5 V at pH 9.2 and 14 using a laminar flux double channel electrode flow cell (DCEFC). An E/pH diagram, especially built for this work, indicates that the surface of the mineral is stable between these potentials but can be oxidized to CuS and $Fe(OH)_3$ at $E > -0.1$ V or reduced to Cu_2S, FeS and S^{2-} at $E < -0.5$ V. The results show that oxygen is reduced to peroxide ion, HO_2^-. At pH 9.2 the generated sulphide ions hinder the oxidation of HO_2^- on the collector electrode of the DCEFC, due to the formation of a blocking surface layer of elemental sulphur, S, which impedes the determination of the kinetic parameters of the oxygen electroreduction reaction. In contrast, at pH 14, soluble polysulphides are formed, and can be determined. At this pH, the electroreduction of oxygen on bornite occurs predominantly with formation of HO_2^-, as $n_g = 2$ and $k_1/k_2 < 1$. The smaller magnitudes of the kinetic constants k_1 and k_2 show that the mineral surface behaves as a poor electrocatalyst for oxygen reduction.

At pH 14, and in the presence of ethylxanthate, the ethylxanthate ion is oxidized by HO_2^- to perxanthate and monothiocarbonate ions, which should have a detrimental effect on the efficiency of the mineral concentration by flotation. However, at pH 9.2, due to the fact that a hydrophobic xanthate layer should be adsorbed on the mineral surface, the flotation efficiency would be higher than at more alkaline pH.

Acknowledgements

The present work is part of the French-Chilean Scientific Coöperation (UPL/USACH Convention and

PICS/CNRS). J.O. and J.L.G. acknowledge the financial support of DICYT–USACH and the suggestions of the referee.

References

[1] R. Woods, IV Meet. of the South. Hemisph. on Mineral Tech. and III Latinam. Congress on 'Froth Flotation' (edited by S. Castro, J. Alvarez) (1994), p. 1.
[2] T. Biegler, D. A. J. Rand and R. Woods, *J. Electroanal. Chem.* **60** (1975) 151.
[3] I. N. Plaskin and S. V. Bessonov, Proceedings of the 2nd International Congress 'Surface Activity', Vol. 3 (1957), p. 361.
[4] E. Yeager, *Electrochim. Acta* **29** (1984) 1527.
[5] W. J. Albery and M. L. Hitchman, 'Ring-Disc Electrodes', Clarendon Press, Oxford (1971), pp. 17–28.
[6] R. G. Compton and P. R. Unwin, *J. Electroanal. Chem.* **205** (1986) 1.
[7] M. H. Jones and J. T. Woodcock, *Int. J. Miner. Process* **5** (1978) 285.
[8] G. Berglund and E. Forssberg, 1988 Proceedings of the International Symposium on Electrochemistry in Mineral Processes II (edited by P. E. Richardson, and R. Woods), Vol. 88-21, p. 183.
[9] R. Woods, C. I. Basilio, D. S. Kim and R. H. Yoon, *Int. J. Miner. Process.* **42** (1994) 215.
[10] N. Heller-Ling, G. Poillerat, J. F. Koenig, J. L. Gautier and P. Chartier, *Electrochim. Acta* **39** (1994) 1669.
[11] A. N. Buckley, I. C. Hamilton and R. Woods, *J. Appl. Electrochem.* **14** (1984) 63.
[12] J. B. Zachwieja, G. W. Walker and P. E. Richardson, *Miner. Metall. Process.* 4(3) (1987) 146
[13] M. Pourbaix, 'Atlas of Electrochemical Equilibria in Aqueous Solutions', Nace-Cebelcor. Brussels.(1974) pp. 98, 308, 385 and 546.
[14] D. A. J. Rand, *J. Electroanal. Chem.* **83** (1977) 19.
[15] R. J. Biernat and R. G. Robins, *Electrochim. Acta* **17** (1972) 1261.
[16] R. Woods, R. H. Yoon and C. A. Young, *Int. J. Min. Proc.* **20** (1987) 109.
[17] D. F. A. Koch and R. Mc. Intyre, *J. Electroanal. Chem.* **71** (1976) 285.
[18] J. Szynkarczuk, P. G. Komorowski and J. C. Donini, *Electrochim. Acta* **40** (1995) 487.
[19] H. S. Wroblowa, Y. C. Pan and G. Razumney, *J. Electroanal. Chem.* **69** (1976) 195.
[20] R. W. Zurilla, R. K. Sen and E. Yeager, *J. Electrochem. Soc.* **125** (1978) 1103.
[21] A. J. Appleby and M. Savy, *J. Electroanal. Chem.* **92** (1978) 15.
[22] H. Behret, H. Binder, W. Clauberg and G. Sandstede, *Electrochim. Acta* **23** (1978) 1023.
[23] V. S. Vilinskaya, N. G. Bulavina, V. Y. Shepelev and R. K. H. Burshtein, *Elektrokhimiya* **15** (1979) 932.
[24] F. Van Den Brink, W. Visscher and E. Barendrecht, *J. Electroanal. Chem.* **172** (1984) 301.
[25] S. Park, S. Ho, S. Aruliah, M. F. Weber, C. A. Ward, R. D. Venter and S. Srinivasan. *J. Electrochem. Soc.* **133** (1986) 1641.
[26] V. Jovancicevic and J. O'M. Bockris, *Ibid.* **133** (1986) 1797.
[27] J. L. Gautier, A. Restovic and P. Chartier. *J. Appl. Electrochem.* **19** (1989) 28.
[28] N. Anastasijevic, Z. M. Dmiitrijevic and R. R. Adzic. *Electrochim. Acta* **27** (1992) 457.
[29] S. Strbac, N. A. Anastasijevic and R. R. Adzic, *J. Electroanal. Chem.* **323** (1992) 179.
[30] J. Ortiz and J. L. Gautier, *Ibid.* **391** (1995) 111.
[31] N. Heller-Ling, M. Prestat, J. L. Gautier, J. F. Koenig, G. Poillerat and P. Chartier, *Electrochim. Acta* **42** (1997) 197.
[32] I. C. Hamilton and R. Woods. *J. Appl. Electrochem.* **13** (1983) 783.
[33] A. C. Buckley, I. C. Hamilton and R. Woods, *J. Electroanal. Chem.* **216** (1987) 213.
[34] D. Bauer, M. Lamache, O. Huynh Thi, *Electrochim. Acta* **26** (1981) 33.
[35] R. Woods, *J. Phys. Chem.* **75** (1971) 354.
[36] A. H. Usul, R. Tolun, *Int. J. Min. Proc.* **1** (1974) 135.
[37] R. N. Tipman and J. Leja, *Colloid and Polymer Sci.* **253** (1975) 4.
[38] M. H. Jones and J. T. Woodcock, *Int. J. Min. Proc.* **10** (1983) 1.